C.P. No. 877

MINISTRY OF AVIATION

AERONAUTICAL RESEARCH COUNCIL

CURRENT PAPERS

The Flapping Behaviour of a Helicopter Rotor at High Tip-Speed Ratios

by

E. Wilde, Ph.D. A. R. S. Bramwell, M.Sc. Ph.D.

and

R. Summerscales, B.Sc.

LONDON: HER MAJESTY'S STATIONERY OFFICE

1966

PRICE 7*s* 6*d* NET

U.D.C. No. 533.662.6 : 533.6.013.42

C.P. No.877

April 1965

THE FLAPPING BEHAVIOUR OF A HELICOPTER ROTOR AT HIGH TIP-SPEED RATIOS

by

E. Wilde, Ph.D.
A. R. S. Bramwell, M.Sc. Ph.D.
R. Summerscales, B.Sc.

SUMMARY

The blade flapping equation has been solved on an analogue computer taking into account the reversed flow region but neglecting stall. The fully articulated blade becomes unstable at about $\mu = 2.3$, whilst a see-saw rotor is stable up to $\mu = 5$ at least and the trends suggest that it may be stable for all values of μ. However, the response to a gust, or the equivalent change of no-feathering axis angle, is almost the same for both rotors up to about $\mu = 0.75$. For a 35 ft/sec gust at a forward speed of 200 ft/sec, and typical rotor/fuselage clearance, this represents the limiting tip-speed ratio for either rotor. The better response of the see-saw rotor, however, makes it possible to increase the limiting tip-speed ratio by some form of flapping restraint. This has been investigated by considering the effects of springs and dampers, and offset and δ_3-hinges.

Replaces R.A.E. Technical Report 65068 - A.R.C. 27375

CONTENTS

1 INTRODUCTION

Rotorcraft have established themselves as flight vehicles of great utility but with low top speed. This utility would be improved if the top speed could be increased and considerable attention has already been devoted to basic performance assessments. This work has indicated that significant improvements are possible but more detailed consideration of rotor characteristics, such as blade flapping amplitudes and stability, is essential before the improvement can be completely determined.

In order to reduce compressibility losses and noise, it will be necessary to reduce the speed of the rotor as the forward speed increases. This means that the tip speed ratio, μ, will become high and might even exceed unity. Little is known about blade flapping stability at these high values of μ as the flapping equation has periodic coefficients and is extremely difficult to solve analytically. Several attempts to obtain solutions have been made, the most recent being those of Shutler and Jones[1] and Lowis[2]. In all these attempts the aerodynamic flapping moment from the region of reversed flow was not merely ignored but had to appear with the wrong sign in order that the flapping moment should be correct in the more important advancing region*. This would not be important at low values of μ but would result in serious error at the very values of μ for which the investigation was required.

With the aid of an analogue computer, the reversed flow region has now been included in an investigation of blade flapping behaviour and the results are described in this paper. Both freely flapping and see-saw rotors have been analysed and the effects of springs, dampers and δ_3- and offset hinges have been considered.

2 THE FREELY FLAPPING ROTOR

2.1 Analysis of the fully articulated rotor

The rotor divides itself into three regions as shown in Fig.1. They are:-

(1) The "advancing" region where the airflow over the whole blade is from leading edge to trailing edge, $0 \leq \psi \leq \pi$.

---

* While the work described in this Report was in progress another paper by Lowis[3] appeared in which the reversed flow region was approximately taken into account. His results largely confirm some of the findings of this Report.

(2) The "partial reverse" region where the airflow is from leading to trailing edge over the outboard part of the blade, but from trailing to leading edge over the inboard part. When $\mu \leq 1$ this region extends from $\psi = \pi$ to $\psi = 2\pi$. When $\mu > 1$ the region is in two parts given by $-\frac{1}{\mu} \leq \sin\psi \leq 0$.

(3) The "total reversed" region which exists when $\mu > 1$ and the flow is from trailing edge to leading edge over the whole span. In this region $\sin\psi < -\frac{1}{\mu}$.

The aerodynamic moment will be determined in each of these regions subject to the following assumptions.

(1) The lift slope is constant and has the same value for both advancing and reversed flow.

(2) The effects of stalling and compressibility are ignored. Compressibility would be avoided in practice and so the latter assumption is not unreasonable. The assumption of no stalling leads to great simplifications and since many of the cases of interest involve lightly loaded rotors, this assumption would appear to be justified.

(3) The effect of spanwise flow is neglected.

(4) Unsteady aerodynamic effects are ignored.

The system of axes is shown in Fig.2.

The velocity at a blade section distance r from the root, in a plane perpendicular to the no-feathering axis has a chordwise component, U_T, given by

$$U_T = \Omega r + V \cos\alpha_{nf} \sin\psi$$

or

$$U_T = \Omega R\,(x + \mu \sin\psi) \qquad (1)$$

where $\mu = \dfrac{V \cos\alpha_{nf}}{\Omega R}$

The velocity at a blade section, parallel to the no-feathering axis, is

$$U_p = V \sin\alpha_{nf} - v_i - V\beta \cos\alpha_{nf} \cos\psi - r\dot{\beta}$$

$$= \Omega R\,(\lambda - \mu\beta \cos\psi - x\dot{\beta}/\Omega) \qquad (2)$$

where $\lambda = \dfrac{V \sin\alpha_{nf} - v_i}{\Omega R}$

If the collective pitch is θ_o, and the airflow is from leading to trailing edge, then the incidence of the element is

$$\alpha = \theta_o + \tan^{-1}\left(\frac{U_P}{U_T}\right) \simeq \theta_o + \frac{U_P}{U_T} \tag{3}$$

Assuming $C_L = a\alpha$, the lift on an element of blade length dr is

$$dL = \frac{1}{2}\rho a c U_T^2 \left(\theta_o + \frac{U_P}{U_T}\right) dr .$$

The elementary lift moment is

$$dM = \frac{1}{2}\rho a c U_T^2 \left(\theta_o + \frac{U_P}{U_T}\right) r dr \tag{4}$$

Substituting equations (1) and (2) into (4) and integrating from x = 0 to x = 1 gives for the advancing region,

$$\frac{M_{AR}}{I\Omega^2} = \frac{\gamma}{2}\left\{\frac{1}{4}\theta_o + \frac{2}{3}\mu\theta_o \sin\psi + \frac{1}{2}\mu^2\theta_o \sin^2\psi + \frac{1}{3}\lambda - \frac{1}{3}\mu\beta\cos\psi - \frac{1}{4}\frac{\dot{\beta}}{\Omega}\right.$$
$$\left. + \frac{1}{2}\mu\lambda\sin\psi - \frac{1}{2}\mu^2\beta\sin\psi\cos\psi - \frac{1}{3}\mu\frac{\dot{\beta}}{\Omega}\sin\psi\right\} \tag{5}$$

where M_{AR} denotes the blade flapping moment in the advancing region.

When the flow is from trailing edge to leading edge the expression for α in equation (3) changes sign, i.e.

$$\alpha = -\left(\theta_o + \frac{U_P}{U_T}\right) \tag{6}$$

In the "partial reverse" region, therefore, we use expression (6) between $x = 0$ and $x = -\mu\sin\psi$ and expression (3) from $x = -\mu\sin\psi$ to $x = 1$. Thus if M_{PR} is the flapping moment in the partial reverse region,

$$M_{PR} = -\frac{1}{2}\rho a \int_{0}^{-\mu \sin\psi} c\, U_T^2 \left(\theta_o + \frac{U_P}{U_T}\right) r dr + \frac{1}{2}\rho a \int_{-\mu \sin\psi}^{1} c\, U_T^2 \left(\theta_o + \frac{U_P}{U_T}\right) r dr \quad (7)$$

But equation (7) can be rewritten as

$$M_{PR} = \frac{1}{2}\rho a \int_{0}^{1} c\, U_T^2 \left(\theta_o + \frac{U_P}{U_T}\right) r dr - \rho a \int_{0}^{-\mu \sin\psi} c\, U_T^2 \left(\theta_o + \frac{U_P}{U_T}\right) r dr$$

$$= M_{AR} - \rho a \int_{0}^{-\mu \sin\psi} c\, U_T^2 \left(\theta_o + \frac{U_P}{U_T}\right) r dr$$

$$= M_{AR} - \frac{\gamma I \Omega^2}{12} \mu^3 \sin^3\psi \left(\mu \theta_o \sin\psi + 2\lambda - 2\mu\beta\cos\psi + \frac{\mu\dot{\beta}}{\Omega}\sin\psi\right) \quad (8)$$

Finally, if M_{TR} is the flapping moment in the "total reverse" region, we have, since equation (6) applies along the entire blade,

$$M_{TR} = -M_{AR} \quad (9)$$

The equation of the flapping motion is

$$\beta'' + \beta = \frac{M}{I\Omega^2} \quad (10)$$

where the dashes denote differentiation with respect to ψ and M stands for either M_{AR}, M_{PR}, M_{TR} according to which region the blade is in, as described above.

Equation (10) is very difficult to solve analytically because some of the coefficients are periodic and because the forms of M depend on the values of the independent variable ψ. However, these difficulties are easily overcome in an analogue computer since the periodic coefficients can be handled by multiplier units whilst electronic relays can be arranged to switch in the correct moment terms at the appropriate values of ψ. The program used is given in Appendix A.

2.2 The analysis of the see-saw rotor

The flapping motions of the blades of a see-saw rotor are no longer independent, since the blades are structurally integral but jointly free to flap. The flapping equation may be found by the same methods as before but this time the rotor disc is divided into four regions as shown in Fig.3. These regions are:-

(1) Where the airflow over the reference blade is from leading to trailing edge but over the other blade it is partially reversed. In this region $0 < \sin\psi < \frac{1}{\mu}$.

(2) Where the airflow over the reference blade is from leading to trailing edge but over the other blade it is totally reversed. This occurs only if $\mu > 1$ and when $\frac{1}{\mu} < \sin\psi$.

(3) Where the airflow over the reference blade is partially reversed but over the other blade it is from leading to trailing edge. For this case $-\frac{1}{\mu} < \sin\psi < 0$.

(4) Where the airflow over the reference blade is totally reversed but over the other blade it is from leading to trailing edge. Again, this occurs only if $\mu > 1$ and when $\sin\psi < -\frac{1}{\mu}$.

If the built-in coning angle is a_o, then the flapping of the referecce blade will be $a_o + \beta$ and of the other blade $a_o - \beta$. The flapping moments for the complete see-saw rotor for the four regions then become:-

when $$0 < \sin\psi < \frac{1}{\mu}$$

$$\begin{aligned}\frac{M_{A_1}}{I\Omega^2} = \frac{\gamma}{2}\Big\{&\frac{2}{3}\mu\theta_o\sin\psi - \frac{1}{3}\mu a_o\cos\psi + \frac{1}{2}\mu\lambda\sin\psi + \frac{1}{12}\theta_o\mu^4\sin^4\psi \\ &- \frac{1}{6}\mu^3\lambda\sin^3\psi - \frac{1}{6}\mu^4 a_o\sin^3\psi\cos\psi\Big\} \\ &- \frac{\gamma}{2}\beta\left\{\frac{1}{2}\mu^2\sin\psi\cos\psi - \frac{1}{6}\mu^4\sin^3\psi\cos\psi\right\} \\ &- \frac{\gamma}{2}\beta'\left\{\frac{1}{4} + \frac{1}{12}\mu^4\sin^4\psi\right\} \qquad (11)\end{aligned}$$

when $$\frac{1}{\mu} < \sin\psi\ ,$$

$$\frac{M_{A_2}}{I\Omega^2} = \frac{\gamma}{2}\left\{\frac{1}{4}\theta_o + \frac{1}{2}\mu^2\theta_o \sin^2\psi + \frac{1}{3}\lambda - \frac{1}{2}\mu^2 a_o \sin\psi\cos\psi\right\}$$

$$- \frac{\gamma}{6}\beta\,\mu\cos\psi - \frac{\gamma}{6}\beta'\,\mu\sin\psi \qquad (12)$$

when $$-\frac{1}{\mu} < \sin\psi < 0\ ,$$

$$\frac{M_{A_3}}{I\Omega^2} = M_{A_1} - \frac{\gamma}{12}\mu^4 \sin^3\psi\left(\theta_o \sin\psi - 2a_o\cos\psi\right) \qquad (13)$$

when $$\sin\psi < -\frac{1}{\mu}\ ,$$

$$M_{A_4} = -M_{A_2} \qquad (14)$$

3 ANALOGUE COMPUTER RESULTS

3.1 The fully articulated rotor

The computed response to a disturbance of the fully articulated rotor is given in Fig.4. It can be seen that the flapping motion is stable for values of μ up to about 2.25, (depending slightly on Lock's inertia number γ) and becomes unstable at higher values of μ. This is in contrast to the result given by simple theory, which neglects the reversed flow region, and which predicts flapping instability at $\mu = \sqrt{2}$.

The steady blade flapping angles have been computed for a number of values of α_{nf} and for values of μ of 0.35, 0.5, 0.7, 1.0. 1.5 and 2.0. It may be noted that since the differential equation for flapping is linear and the right hand side of the equation is linear in α_{nf}, there must be a linear relationship between β and α_{nf}.

For the freely flapping rotor, the total flapping amplitude, at various values of tip-speed ratio, is plotted against α_{nf} in Fig.5. The coefficients of the first harmonics of flapping, a_1 and b_1 are shown in Fig.6.

In Fig.5 there are shown three curves which give the flapping resulting from a 35 ft/sec gust, under different conditions of flight the collective pitch being assumed to be zero. In one case the gust occurs at a speed of 200 ft/sec

which is assumed to be the speed at which rotor retraction might take place. It can be seen that the flapping exceeds the assumed geometric limit of 9 degrees for μ greater than 0.7. For the other two cases it is assumed that the blade tip Mach number is constant at either 0.85 or 0.95. These assumptions define relationships between α_{nf} and μ which have also been plotted. From these curves it can be seen that the geometric limit is not exceeded for a gust of 35 ft/sec unless μ is greater than about 1, being more or less than 1 according to the tip Mach number. Along each curve there is also a definite variation of forward speed and it appears that the geometric limit is reached at 465 ft/sec when the tip Mach number is 0.85 and 525 ft/sec when it is 0.95.

3.2 The see-saw rotor

The variation of the flapping angle with shaft angle, α_{nf}, for the see-saw rotor is shown in Fig.7. Curves are given for two values of built-in coning angle, 0 degree and 4 degrees. It can be seen that the curves for the 4 degrees coning angle are not linear with α_{nf}. This is to be expected as the coning angle itself will produce flapping even when α_{nf} is zero. The curves of Fig.7 should be compared with those of Fig.5 for the fully articulated rotor. Up to a tip speed ratio of about 0.75 the responses of both rotors are very similar but whereas the freely flapping rotor becomes unstable at about $\mu = 2.3$, the see-saw rotor is stable up to $\mu = 5$ at least. The slope of the curve of flapping with α_{nf}, as a function of μ, is shown in Fig.8 where it can be seen that $d\beta/d\alpha_{nf}$ becomes roughly linear above about $\mu = 1$. For the unrestrained see-saw rotor this is not of great use since the factor limiting its use is the response to a 35 ft/sec gust at about $\mu = 0.7$ which is similar to that of the freely flapping rotor. However, the suppression of flapping at higher values of μ enables values of μ to be reached of between 1.5 and 2, depending on the coning angle, with corresponding forward speeds of at least 600 ft/sec. This latter speed must be accompanied by a very low rotor speed, of course, in order that the tip Mach number should remain at 0.85, or at some value close to this figure.

It has been assumed in the analysis that the blades are perfectly rigid and that the coning angle remains fixed. It is realised, that in practice, the coning angle may differ from the assumed value, due to blade flexibility, by an amount which depends upon the flapping. It is thought, however, that unless the flapping is excessively large, the range of coning angles of Fig.7 will cover most cases of practical interest.

4 RESTRAINT OF FLAPPING MOTION BY SPRINGS AND DAMPERS

Since the amplitude of flapping motion appears to impose operating limits, consideration has been given to various means of restricting it. Springs do not dissipate energy but merely act as stores and consequently will redistribute the flapping. This may be useful, however, in converting backward flapping into sideways flapping since the main obstructions to flapping are in the fore and aft plane. Dampers, on the other hand, actively dissipate energy and so reduce the amount of flapping. It is recognised that such devices may well cause stressing problems but such considerations are beyond the scope of the present investigation.

4.1 Analysis of spring and damper restraint

The spring-damper arrangement considered is shown in Fig.16. As the see-saw rotor appears to have the better stability, only this type of rotor has been considered. However, the method given below is applicable to the freely flapping rotor.

The flapping equation, with spring and damper restraint, can be written

$$2I\ddot{\beta} + I\Omega^2\left(a_o + \beta\right) - I\Omega^2\left(a_o - \beta\right) = M_1 - M_2 - 2\,k_s\,R'^2\,\beta - 2\,k_d\,R'^2\dot{\beta} \qquad (15)$$

where k_s is the spring constant, lb wt/ft

k_d is the damping constant, lb wt/ft/sec

and R' is the distance from the root of the point of attachment.

This equation reduces to

$$\beta'' + \beta = \frac{M_1 - M_2}{2I\Omega^2} - \bar{k}_s\,\beta - \bar{k}_d\,\beta' \qquad (16)$$

where

$$\bar{k}_s = \frac{k_s\,R'^2}{I\Omega^2}$$

$$\bar{k}_d = \frac{k_d\,R'^2}{I\Omega} \qquad (17)$$

Equation (16) implies that the two final terms should be added to equations (11), (12), (13) and (14) to include the effects of spring and damper.

4.2 Computed results

The effects of spring and damper restraint were considered separately. The magnitudes of the spring and damper coefficients were chosen quite arbitrarily merely to illustrate their effects. Owing to the ability of the damper to dissipate energy, a greater range of damper coefficients was considered, so that $\bar{k}_d$ ranged from 0 to 1.4, while $\bar{k}_s$ ranged between 0 and 0.6. Collective pitch and built-in coning angle were kept constant at 0° and 2°, respectively, and tip-speed ratios between 0 and 2.0 were considered. In each case, only a single value of α_{nf} was taken, selected to give convenient scaling on the analogue computer, so that α_{nf} was 8° for $\mu < 1$ and 5° for $\mu > 1$. The results of the computation are shown in Figs. 9–12.

The trends expected in the discussion of Section 4 are confirmed by the results. As indicated above, the ranges of $\bar{k}_d$ and $\bar{k}_s$ were not taken to extreme values but it is not expected that the trends shown would be changed if $\bar{k}_d$ and $\bar{k}_s$ were further increased.

Rough calculations for a typical case show that there may be very large concentrated loads at the points of attachment of spring or damper possibly resulting in unacceptable stresses. However, it is outside the scope of this note to discuss the full structural implications of attaching springs and dampers in the manner shown in Fig.16 or by any other means such as semi-rigid rotors which provide the same restraining moments. The object of the above calculations is merely to show what moments are necessary to reduce the otherwise free flapping to within acceptable limits.

5 RESTRAINT OF FLAPPING MOTION BY MEANS OF A δ_3-HINGE

5.1 The flapping equation

Let I_o be the moment of inertia of the blade about the flapping-hinge when $\delta_3 = 0$ and let I be the moment of inertia for a given value of δ_3.

Then

$$I = I_o \cos^2 \delta_3$$

and the flapping equation is

$$\beta'' + \beta = \frac{M_A}{I_o \cos^2 \delta_3} \qquad (18)$$

With a δ_3-hinge, the incidence of a blade element is

$$\alpha = \theta_o - \beta \tan \delta_3 + \frac{U_P}{U_T} \tag{19}$$

and we get for the flapping moment in the advancing region

$$M_{AR} = \frac{\gamma}{2}\left\{\left(\theta_o - \beta \tan \delta_3\right)\left(\frac{1}{4} + \frac{2}{3}\mu \sin \psi + \frac{1}{2}\mu^2 \sin^2 \psi\right)\right.$$

$$+ \left(\frac{1}{3}\lambda - \frac{1}{3}\mu \beta \cos \psi + \frac{1}{2}\lambda \mu \sin \psi - \frac{1}{2}\mu^2 \beta \sin \psi \cos \psi\right.$$

$$\left.\left. - \frac{1}{4}\beta' - \frac{1}{3}\mu \beta' \sin \psi\right)\right\} \tag{20}$$

As in Section 2.1, when the flow is from trailing edge to leading edge the incidence is reversed and

$$\alpha = -\left(\theta_o - \beta \tan \delta_3 + \frac{U_P}{U_T}\right)$$

The flapping moment for the partially reversed region becomes

$$M_{PRR} = M_{AR} - \frac{I\Omega^2\gamma}{12}\left\{\left(\theta_o - \beta \tan \delta_3\right)\mu^4 \sin^4 \psi - 2\mu^3 \sin^3 \psi \ (\lambda - \mu \beta \cos \psi)\right.$$

$$\left. + \beta' \mu^4 \sin^4 \psi\right\} \tag{21}$$

and for the totally reversed region

$$M_{TRR} = -M_{AR} \tag{22}$$

as before.

The computer program was the same as for the case discussed in 2.1 except for the additional terms in δ_3.

5.2 Computed results

The rate of change of flapping with incidence for a range of μ and δ_3-hinge angles is shown in Fig.13. It can be seen that the effect of the δ_3-hinge

is roughly to reduce the flapping linearly by about 35-40% per 10° of hinge angle over the whole range of μ. Thus, for a 30° hinge, the flapping is reduced to nearly $\frac{1}{3}$ of the flapping when a δ_3- hinge is absent. Fig.14 shows the change in flapping with incidence when $\delta_3 = 30^\circ$ and is to be compared with Fig.4. It can be seen that the operating limit is raised from about $\mu = 1$ to $\mu = 1.5$. The rise in $\partial\beta/\partial\alpha_{nf}$ is so rapid above $\mu = 1.5$ however, that little improvement of operating limit can be expected by increasing the δ_3 angle further.

6 FLAPPING RESTRAINT BY MEANS OF AN OFFSET FLAPPING HINGE

6.1 The flapping equation

The equation of motion of the blade with an offset flapping hinge is

$$I\beta'' + I\beta + M\bar{x}R^2\beta = M_A \tag{23}$$

where I is the moment of inertia about the offset flapping hinge
M is the blade mass
eR is the distance of the flapping hinge from the hub
$\bar{x}R$ is the distance of the centre of gravity of the blade from the flapping hinge.

For a uniform blade of mass m per unit length,

$$\left.\begin{aligned} I &= \tfrac{1}{3}mR^3(1-e)^3 \\ M &= mR(1-e) \\ \bar{x}R &= \tfrac{1}{2}R(1-e) \end{aligned}\right\} \tag{24}$$

and equation (23) reduces to

$$\beta'' + \left\{1 + \frac{3e}{2(1-e)}\right\}\beta = \frac{M_A}{I} \tag{25}$$

The chordwise velocity is the same as in equation (1) but the velocity perpendicular to the blade is now

$$U_P = \Omega R\left[\lambda - \mu\beta\cos\psi - (x-e)\beta'\right] \tag{26}$$

To simplify the calculation of the aerodynamic flapping moment we can put $\theta_o = 0$, since θ_o merely adds a constant to the flapping angle and therefore does not affect the flapping stability or the way in which it varies with the shaft incidence.

Thus

$$M_{AR} = \frac{1}{2} \rho a c \Omega^2 R^4 \int_e^1 \left[\lambda - \mu \beta \cos \psi - (x - e) \beta' \right] \left(x + \mu \sin \psi \right) dx \qquad (27)$$

expanding equation (27) gives

$$M_{AR} = \frac{1}{2} \rho a c \Omega^2 R^4 (1 - e)^3 \left\{ \frac{1}{3} \frac{1 + \frac{1}{2} e}{1 - e} \lambda - \frac{1}{3} \frac{1 + \frac{1}{2} e}{1 - e} \mu \beta \cos \psi \right.$$

$$+ \frac{1}{2} \frac{1}{1 - e} \mu \lambda \sin \psi - \frac{1}{2} \frac{1}{1 - e} \mu^2 \beta \sin \psi \cos \psi$$

$$\left. - \frac{1}{4} (1 + \frac{1}{3} e) \beta' - \frac{1}{3} \mu \beta' \sin \psi \right\}$$

... (28)

therefore

$$\frac{M_{AR}}{I} = \frac{1}{2} \gamma_o \left\{ \frac{1}{3} \frac{1 + \frac{1}{2} e}{1 - e} \lambda - \frac{1}{3} \frac{1 + \frac{1}{2} e}{1 - e} \mu \beta \cos \psi + \frac{1}{2} \frac{1}{1 - e} \mu \lambda \sin \psi \right.$$

$$\left. - \frac{1}{2} \frac{1}{1 - e} \mu^2 \beta \sin \psi \cos \psi - \frac{1}{4} (1 + \frac{1}{3} e) \beta' - \frac{1}{3} \mu \beta' \sin \psi \right\}$$

... (29)

where γ_o is Lock's inertia number for the blade when $e = 0$.

Calculating M_{HRR} in the manner of the previous sections gives

$$M_{HRR} = M_{AR} - \frac{(\mu \sin \psi + e)^3}{12} \left\{ 2\lambda - 2\beta + \beta' (\mu \sin \psi + e) \right\} \qquad (30)$$

and we also have, as before

$$M_{TRR} = - M_{AR} \qquad (31)$$

It will be seen that equations (29), (30) and (31) are of the same form as equations (5), (8) and (9) of Section 2.1, except for the modification of the coefficients.

6.2 Computed results

No computed results are given in the figures as over the whole range of μ the effect of hinge offset on flapping amplitude was found to be very small. As a check on the results from the computer, the values of a_1 and b_1 were calculated for low μ, from the equations of Section 6.1. The results of this calculation are shown in Fig.15 where it can be seen that the total flapping, taken as $(a_1^2 + b_1^2)^{\frac{1}{2}}$, varies only slightly over a large range of hinge offset. Thus, it appears that an offset hinge has practically no effect on blade flapping amplitude, and if anything, tends to increase it. It should be emphasised that the mass per unit length of the blade has been kept constant in the above analysis.

7 STOPPING A ROTOR IN FLIGHT

Performance calculations show that a rotor must be off-loaded to achieve high forward speed which leads one to think about the possibilities of stopping the rotor in forward flight and even of retracting it. One of the main problems of slowing down or stopping a rotor in flight is the loss of centrifugal stiffness which helps to restrain flapping. Although it is possible to reduce the aerodynamic forces on the blade to zero in still air, they may become quite large when there are any atmospheric disturbances.

It is assumed that the speed at which rotor stopping and retraction will occur is about 200 ft/sec. A 35 ft/sec gust at this speed will cause an effective change of disc incidence of 10 degrees and from Figs. 5 and 7 it can be seen that the assumed geometric limit of 9 degrees is reached at about $\mu = 0.7$ for both fully articulated and unrestrained see-saw rotors. From Figs. 7 and 12 it appears that a damper having $\bar{k}_d = 1.2$ will just bring the flapping at $\mu = 2.0$, and coning angle 0 degrees, to within the flapping limit. This means that the rotational speed of a rotor having a 35 foot radius can be reduced to 27 rpm before exceeding $\mu = 2.0$ at 200 ft/sec.

8 CONCLUSIONS

The flapping behaviour of articulated rotors has been investigated up to high values of tip speed ratio, taking into account the region of reversed flow. The conclusions are:-

(1) The motion of a freely flapping rotor becomes unstable at about $\mu = 2.25$, depending a little on Lock's inertia number. The see-saw rotor is stable up to $\mu = 5$ at least and the trend shown by Fig.8 suggests that it may be stable for all μ.

(2) The flapping amplitude in response to a change of disc incidence becomes increasingly great as the tip speed ratio increases. A see-saw rotor has the same tendency but above about $\mu = 1$ it is less than the fully articulated rotor.

(3) The response to a 35 ft/sec gust at 200 ft/sec (assumed speed for rotor retraction) would cause fully articulated blades to strike the fuselage of a typical helicopter configuration at about $\mu = 0.7$. At a cruising speed of 475 ft/sec, corresponding to a tip Mach number of 0.9, a 35 ft/sec gust would cause the blades to strike the fuselage at about $\mu = 1$.

(4) The figures for the see-saw rotor corresponding to (3) above, are $\mu = 0.7$ at a forward speed of 200 ft/sec and $\mu = 1.5$ to 2.0, (depending on the built-in coning angle) when the tip Mach number is 0.9 and the cruising speed is then about 600 ft/sec.

(5) The effect of a δ_3-hinge on a fully articulated blade is roughly to halve the flapping, over the whole range of μ, when the δ_3-angle is 30°. This raises the limiting value of μ to about 1 for the 35 ft/sec gust case at 200 ft/sec. At cruising speed the limiting value of μ is raised from 1 to 1.5, the latter value corresponding to a forward speed of about 600 ft/sec.

(6) An offset hinge has very little effect on the amplitude of blade flapping.

(7) Viscous dampers are quite effective in restraining blade flapping and it appears that little is gained by using springs as well. The structural consequences of using these devices, however, have not been examined.

SYMBOLS

a	local lift slope of blade element
c	blade chord
eR	distance of flapping hinge from centre of rotation
I	moment of inertia of blade about flapping hinge
k_d	damping constant
k_s	spring constant
$\overline{k}_d$	$\frac{k_d R'^2}{I\Omega}$
$\overline{k}_s$	$\frac{k_s R'^2}{I\Omega^2}$
L	lift on a blade
M	moment on blade about flapping hinge
r	distance of blade element from centre of rotation
R	radius of blade
U_P	component of velocity parallel to no-feathering axis
U_T	chordwise component of velocity perpendicular to plane of no-feathering
V	forward speed of helicopter
v_i	induced velocity
α	incidence of blade element
α_{nf}	angle between relative wind and no-feathering axis
β	flapping angle of blade
γ	Lock's inertia number $\frac{\rho a c R^4}{I}$
θ_o	collective pitch angle
λ	inflow ratio, $\frac{V \sin \alpha_{nf} - v_i}{\Omega R}$
μ	tip speed ratio, $\frac{V \cos \alpha_{nf}}{\Omega R}$
ρ	density of air
ψ	blade azimuth angle
Ω	angular velocity of rotor

REFERENCES

No.	Author	Title, etc.
1	A.G. Shutler J.P. Jones	The stability of rotor blade flapping motion. A.R.C. R & M 3178, May 1958
2	O.J. Lowis	The stability of rotor blade flapping motion at high tip speed ratios. A.R.C. 23, 371, January 1962
3	O.J. Lowis	The effect of reverse flow on the stability of rotor blade flapping motion at high tip speed ratios. A.R.C. 24, 431, January 1963

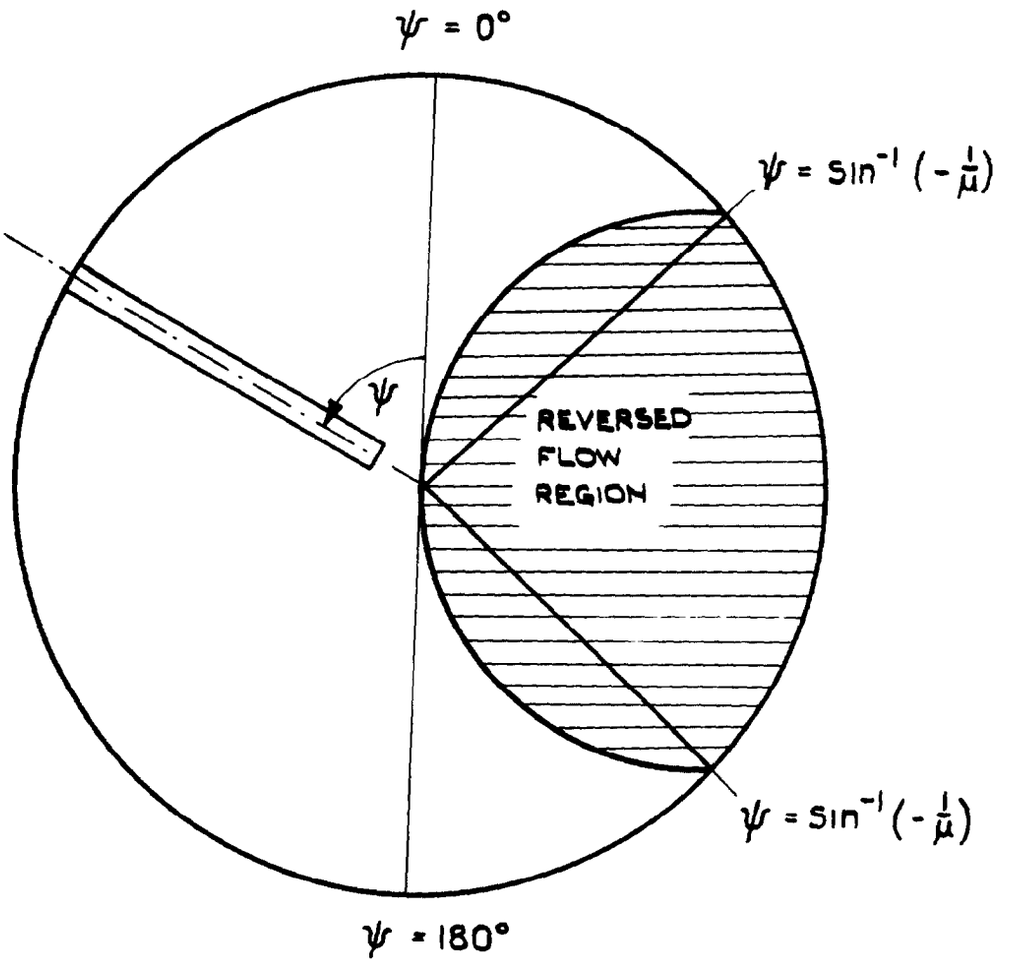

FIG.1 DIAGRAM SHOWING REVERSED FLOW REGION
($\mu > 1$)

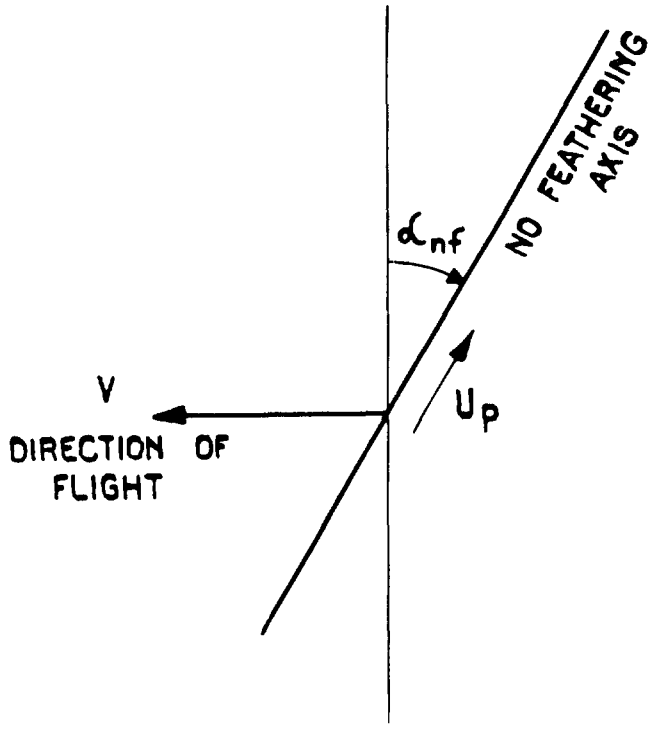

FIG.2(a) RELATION OF NO-FEATHERING AXIS TO DIRECTION OF FLIGHT

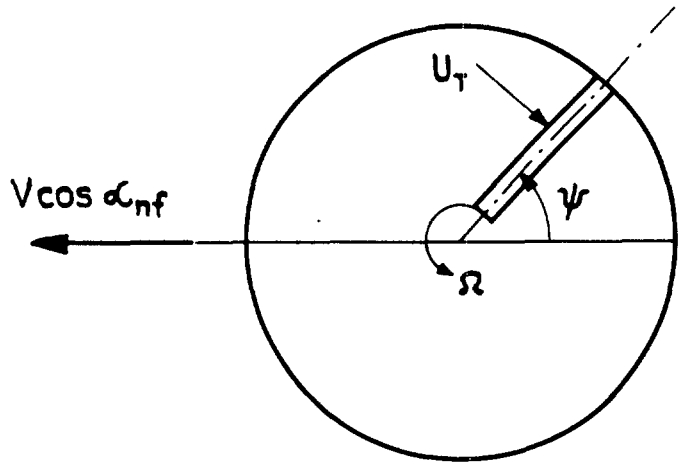

FIG(2b)POSITION OF BLADE IN PLANE PERPENDICULAR TO NO-FEATHERING AXIS.

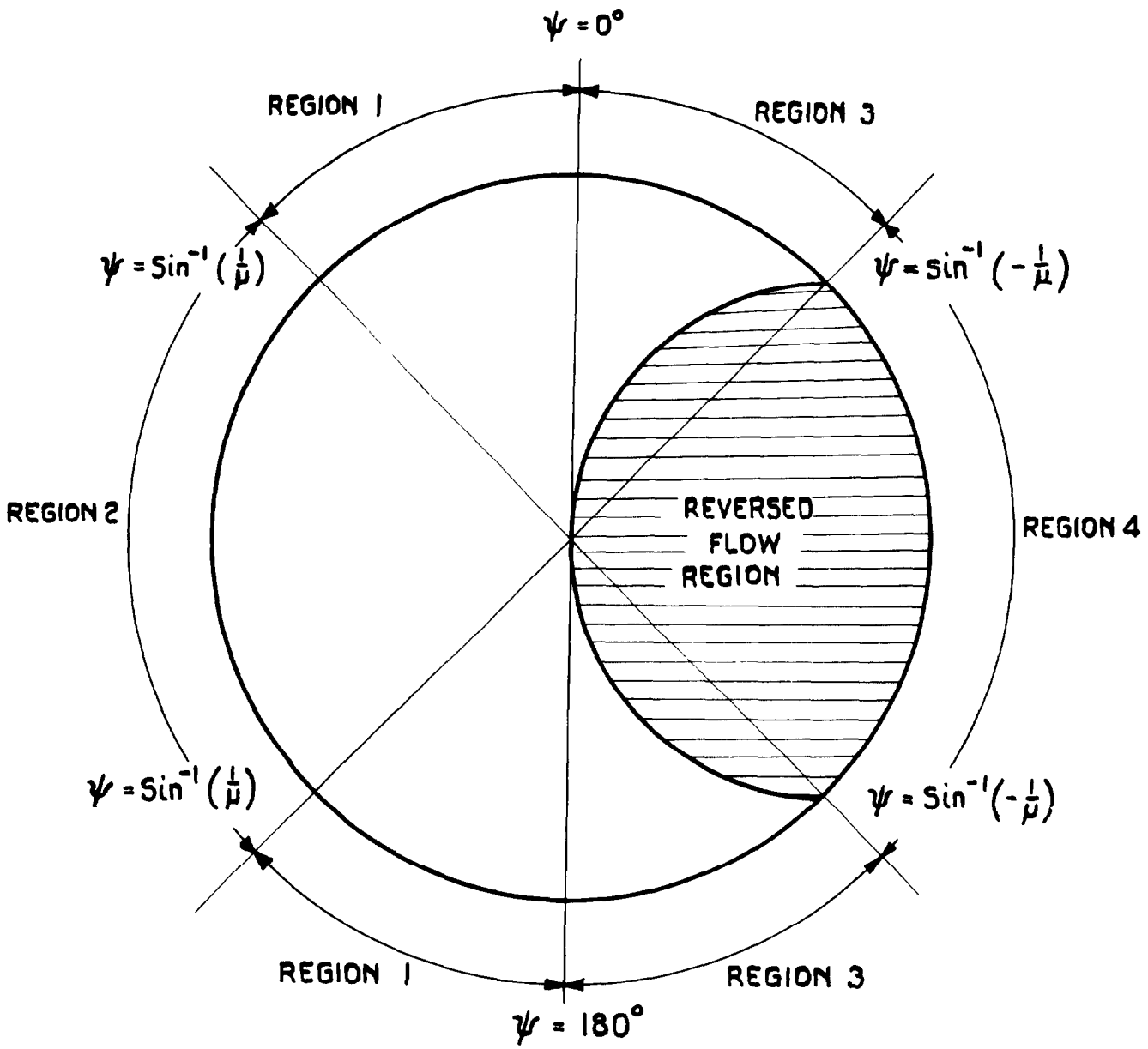

FIG. 3 POSITIONS OF DESIGNATED REGIONS FOR SEE-SAW ROTOR ($\mu = 1{\cdot}5$)

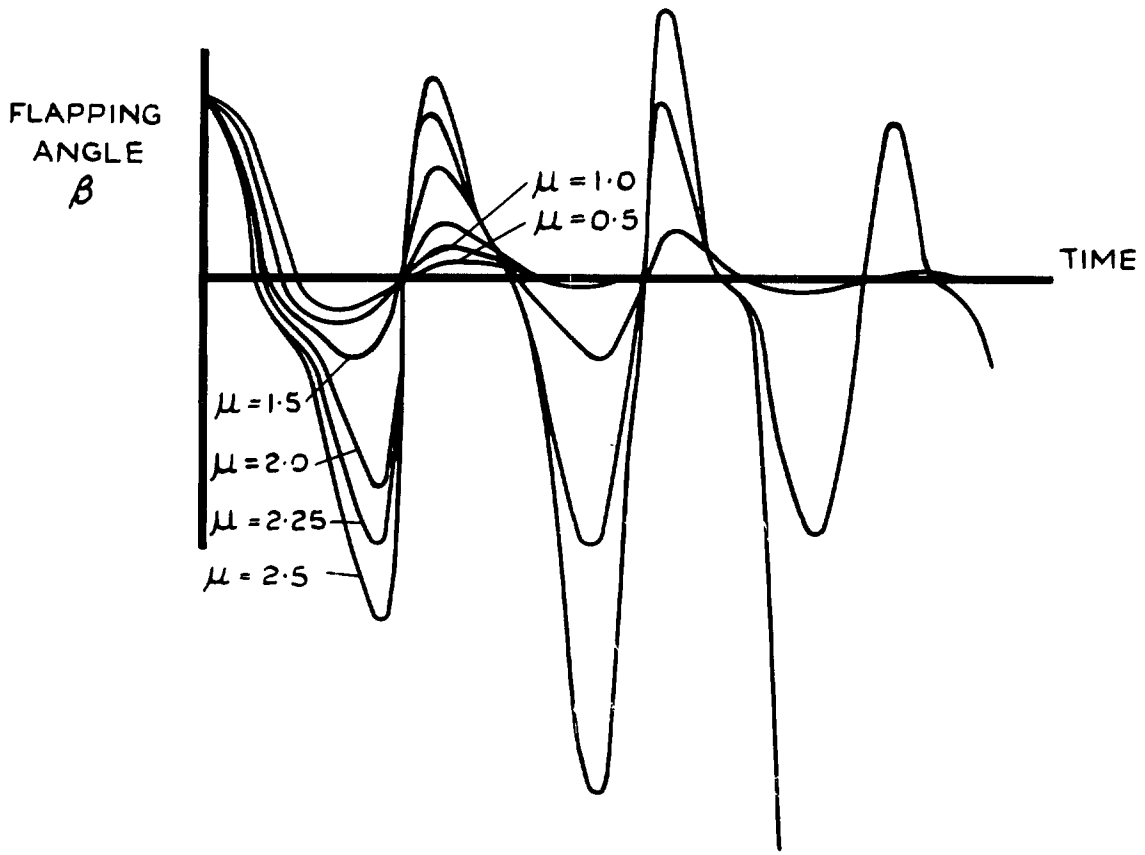

FIG. 4. BLADE FLAPPING STABILITY ($\gamma = 6$)

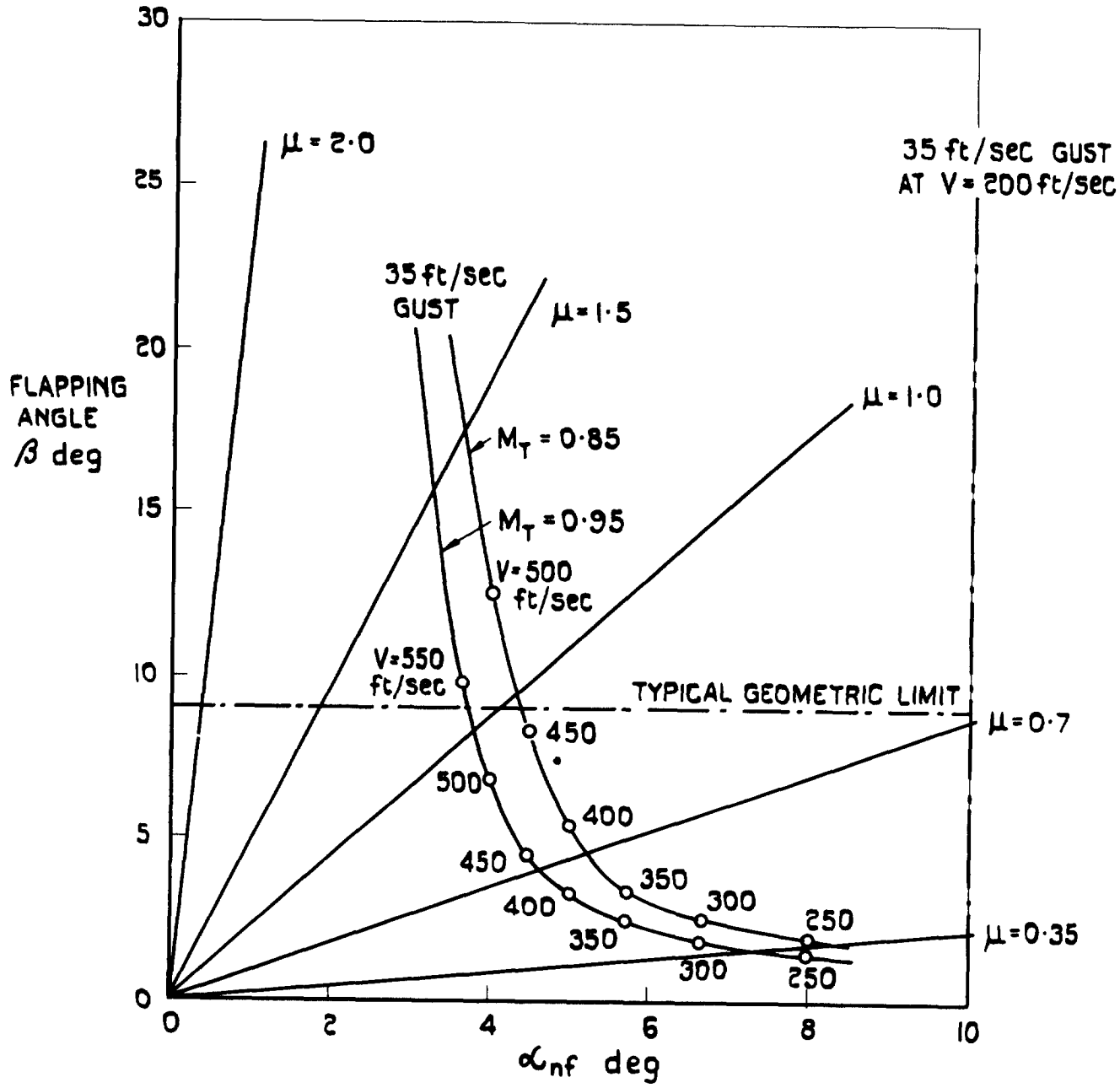

FIG.5 FLAPPING RESPONSE OF FREELY FLAPPING ROTOR TO CHANGE IN ANGLE OF NO-FEATHERING AXIS

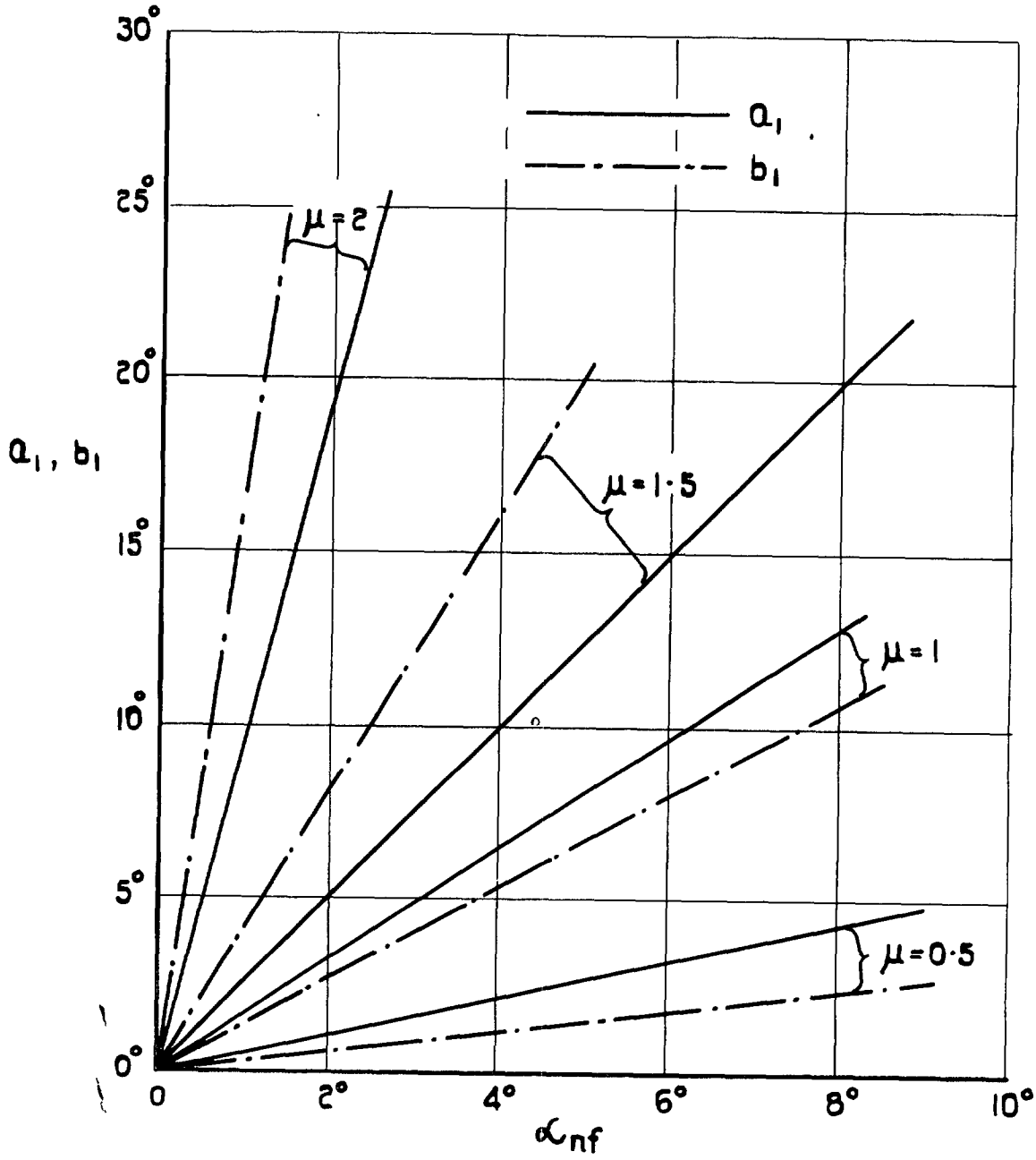

FIG. 6 FIRST HARMONICS OF FLAPPING RESPONSE TO CHANGE IN ANGLE OF NO-FEATHERING AXIS (FREELY FLAPPING ROTOR)

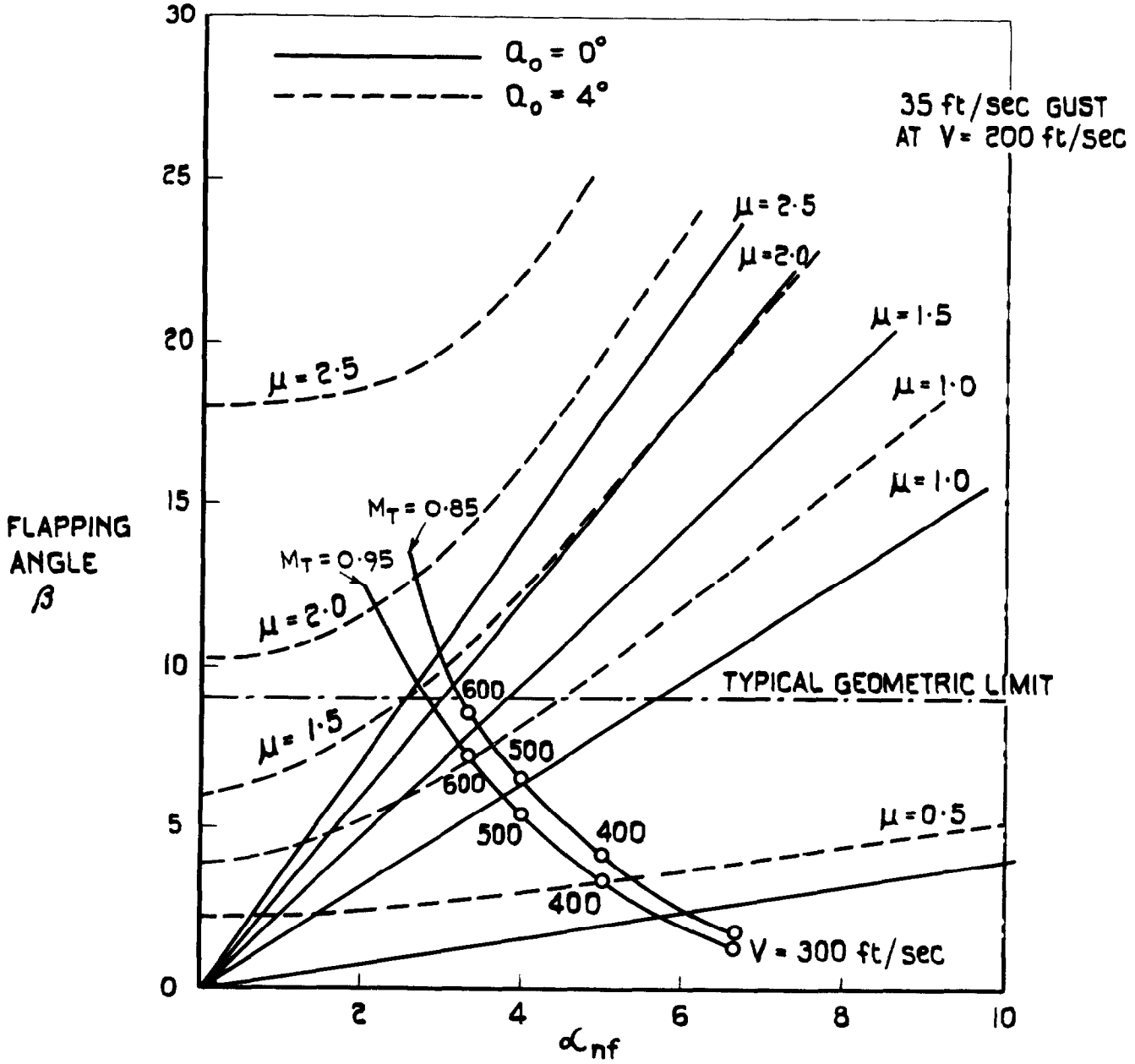

FIG.7 FLAPPING RESPONSE OF A SEE-SAW ROTOR TO CHANGE IN ANGLE OF NO-FEATHERING AXIS

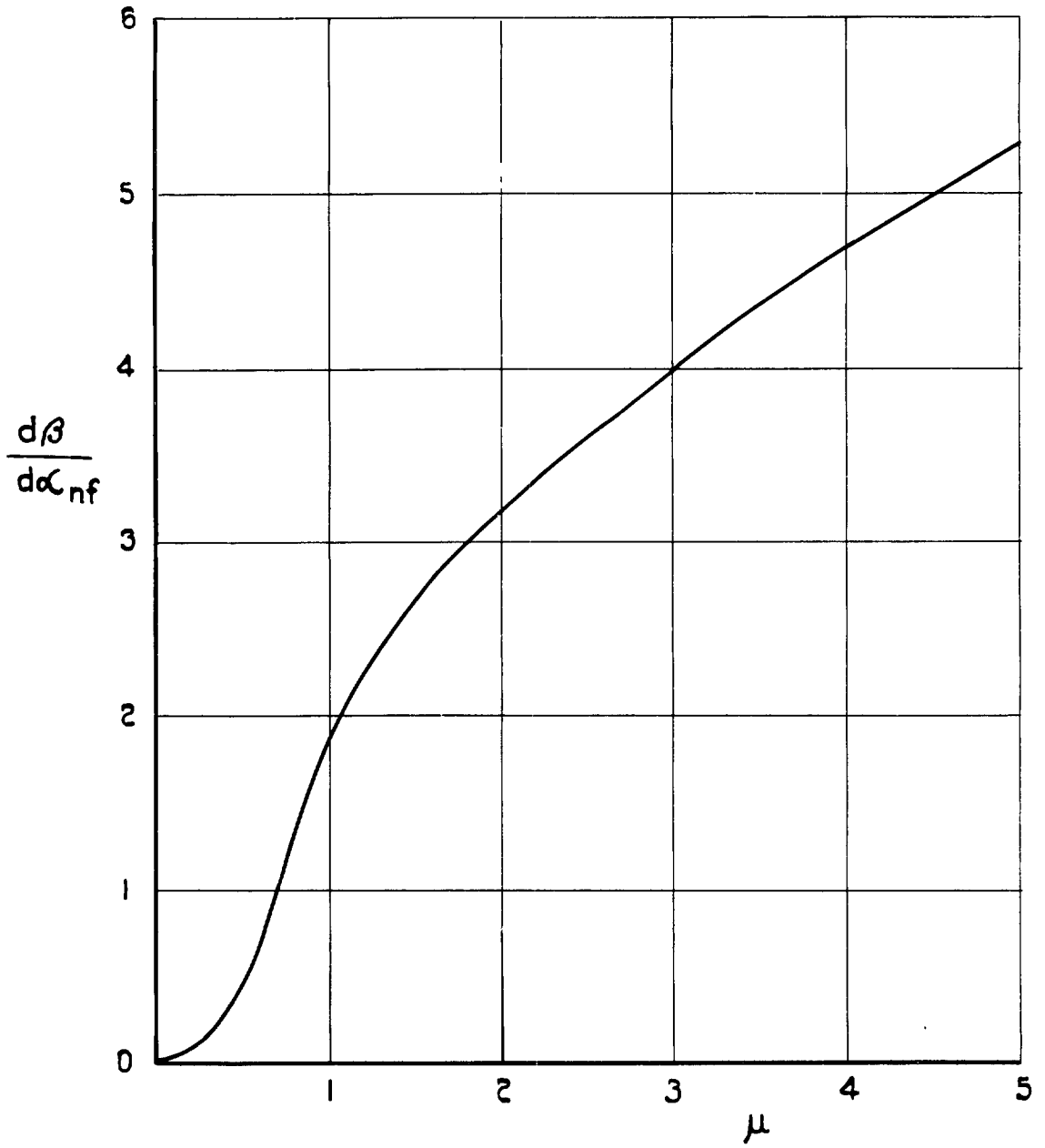

FIG. 8 VARIATION OF $\frac{d\beta}{d\alpha_{nf}}$ WITH μ FOR A SEE-SAW ROTOR $(a = 5{\cdot}6, \gamma = 6)$

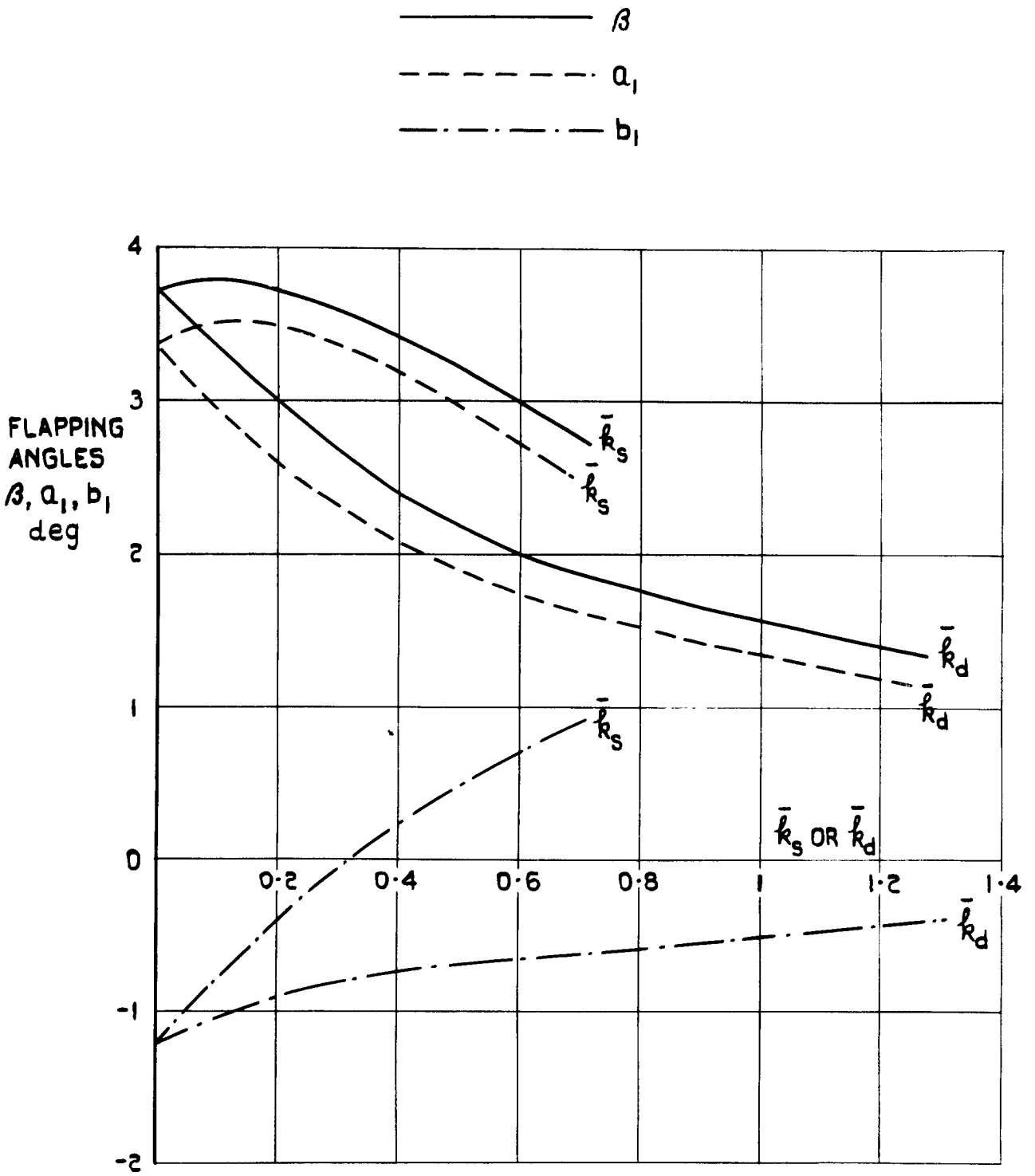

FIG.9 VARIATION OF FLAPPING COEFFICIENTS WITH SPRING AND DAMPER ($\mu = 0.5$, $\alpha_{nf} = 8°$, $a_0 = 2°$, $\theta_0 = 0°$)

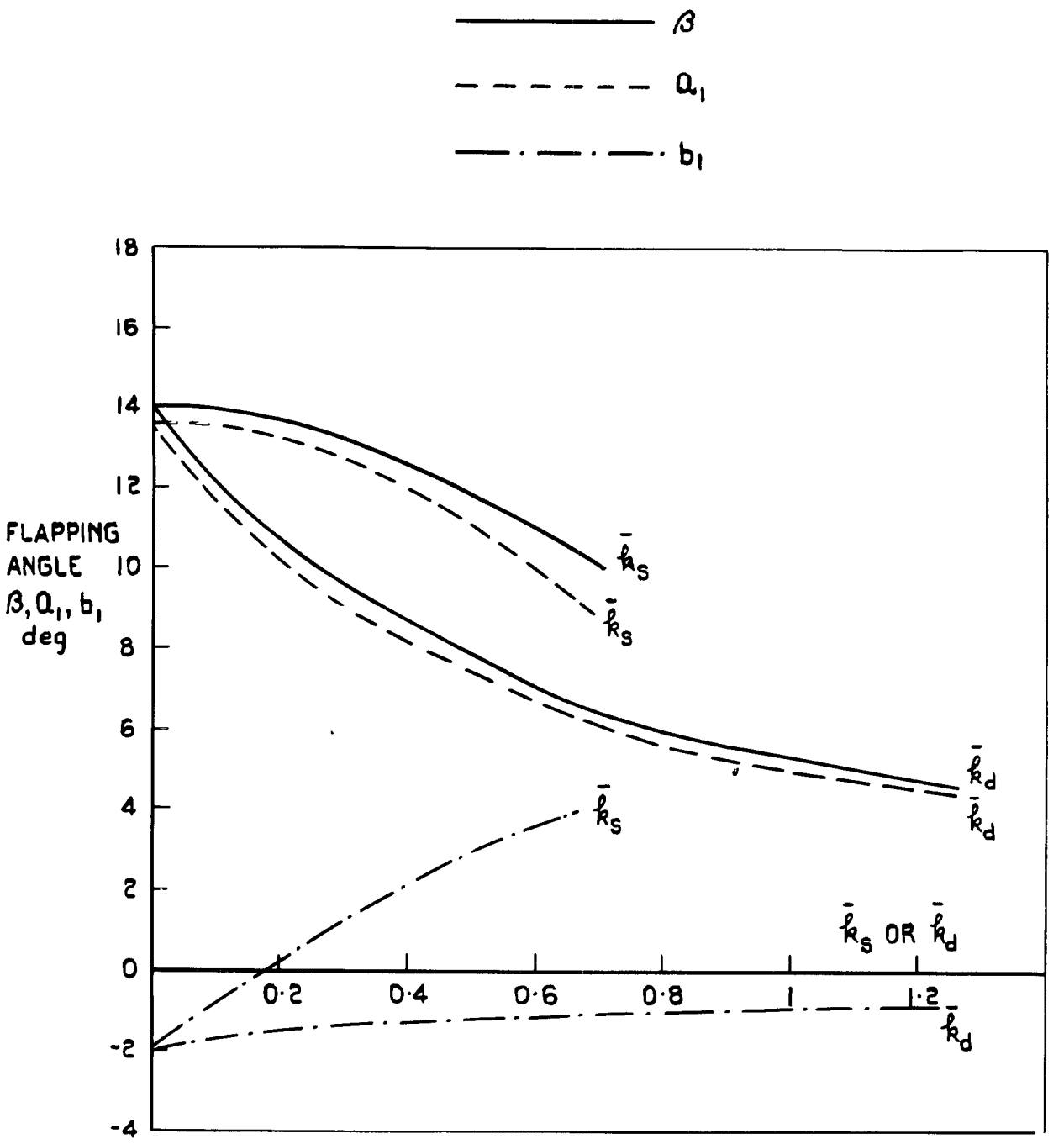

FIG 10. VARIATION OF FLAPPING COEFFICIENTS WITH SPRING AND DAMPER ($\mu = 1$, $\alpha_{nf} = 8°$, $a_0 = 2°$, $\theta_0 = 0°$)

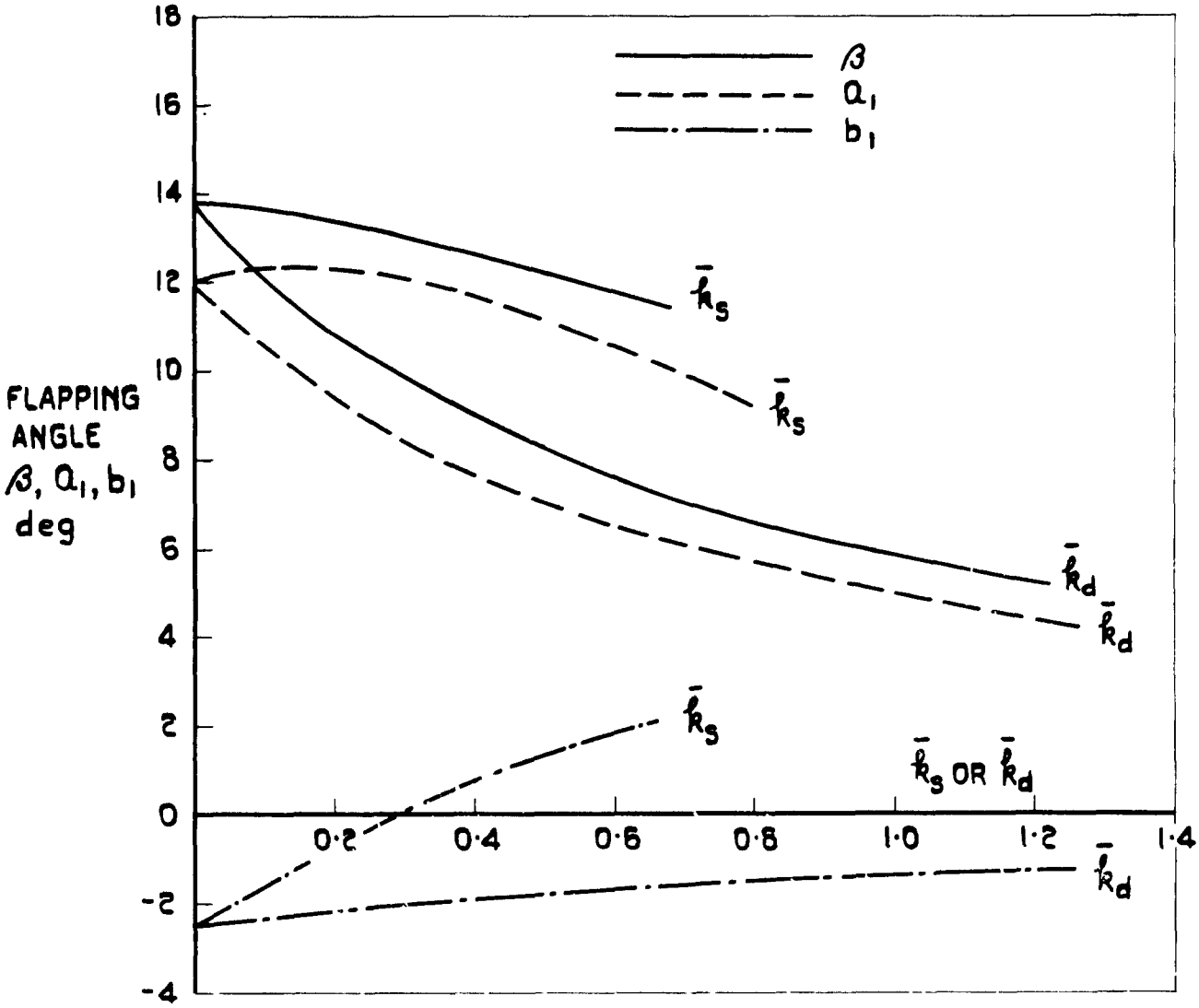

FIG.11 VARIATION OF FLAPPING COEFFICIENTS, WITH SPRING AND DAMPER ($\mu = 1{\cdot}5$, $\alpha_{nf} = 5°$, $a_0 = 2°$, $\theta_0 = 0°$)

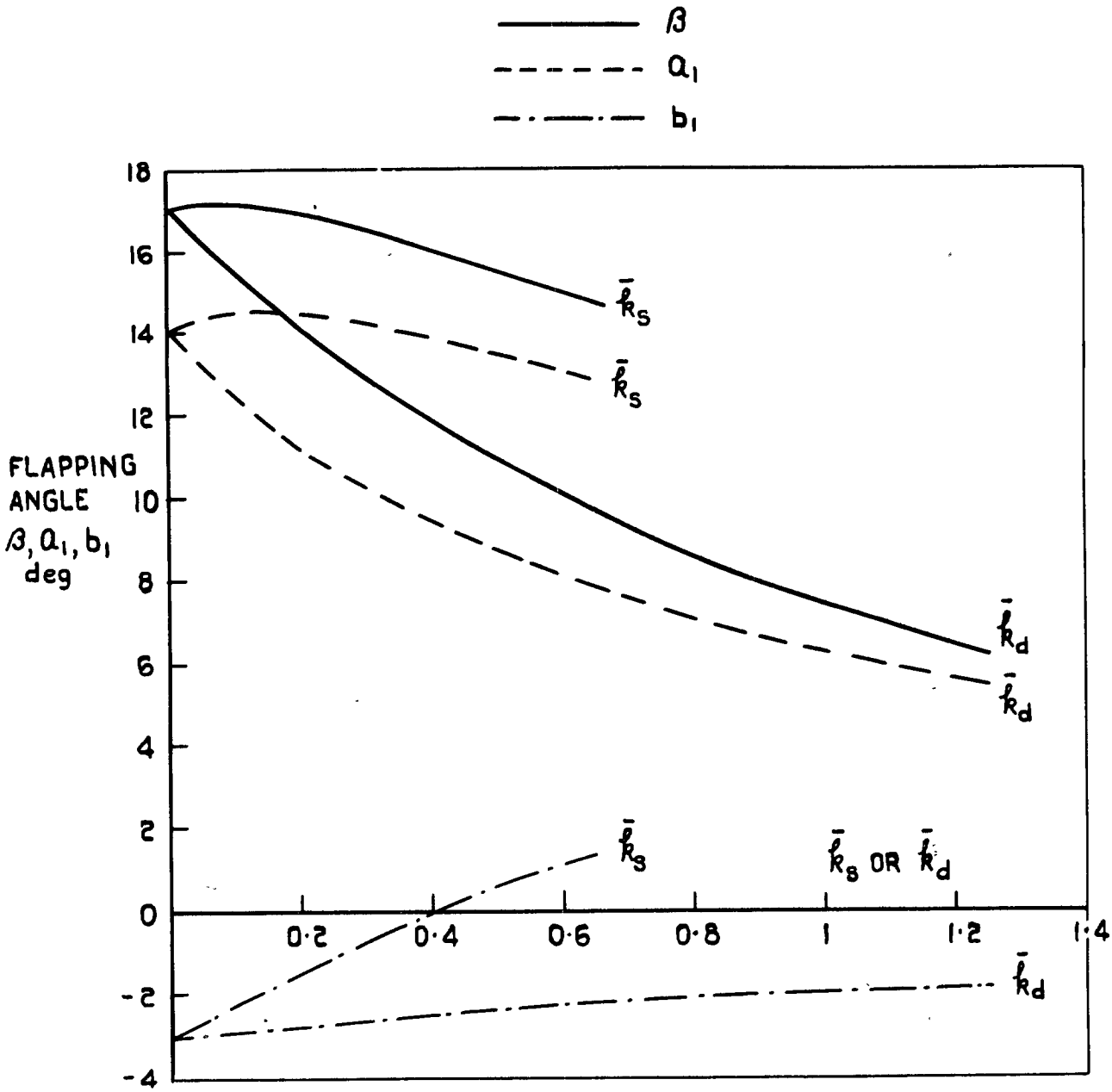

FIG.12. VARIATION OF FLAPPING COEFFICIENTS WITH SPRING AND DAMPER ($\mu = 2$, $\alpha_{nf} = 5°$, $a_0 = 2°$, $\theta_0 = 0°$)

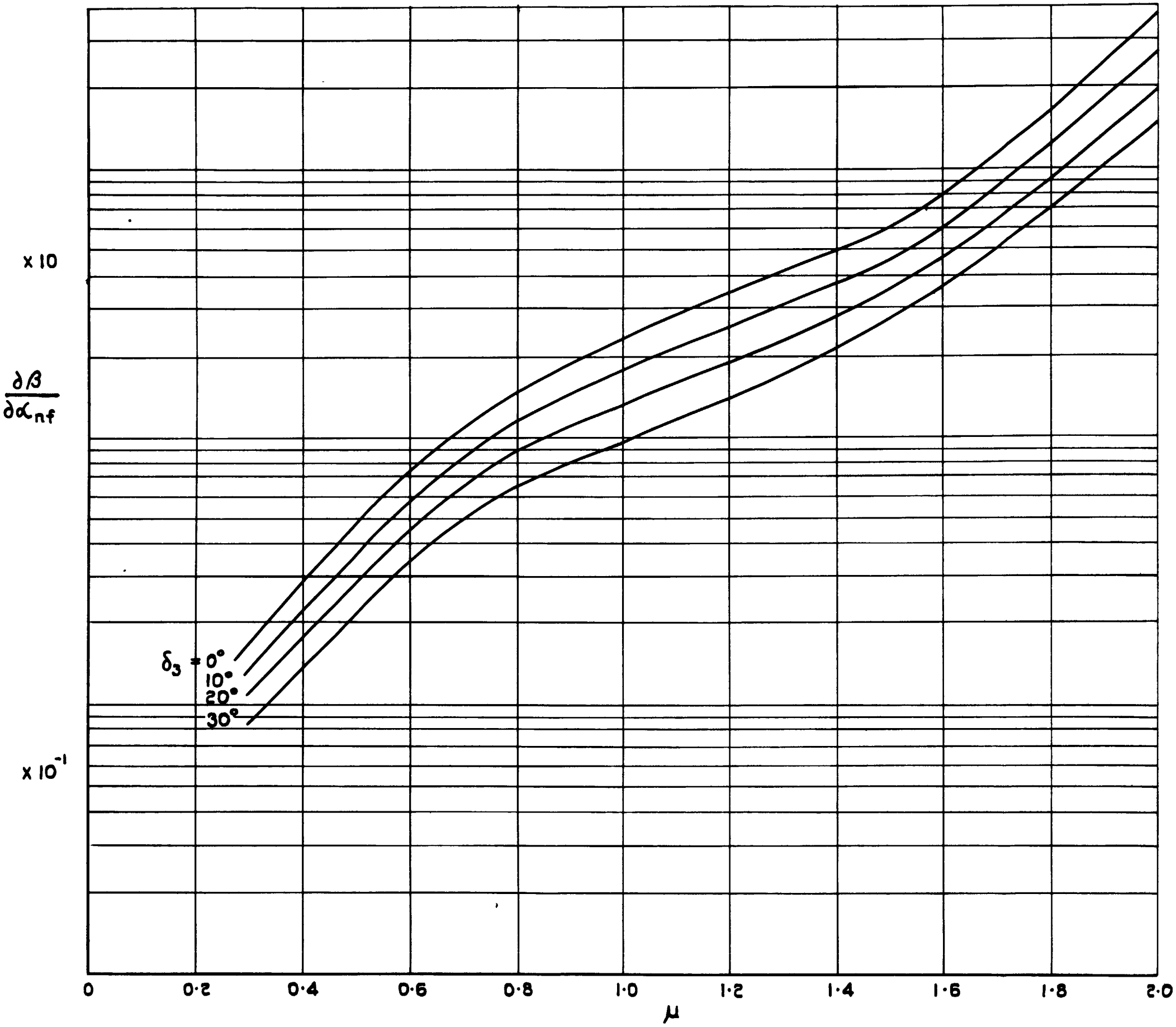

FIG. 13 EFFECT OF δ_3 - HINGE ON RATE OF FLAPPING WITH SHAFT-ANGLE

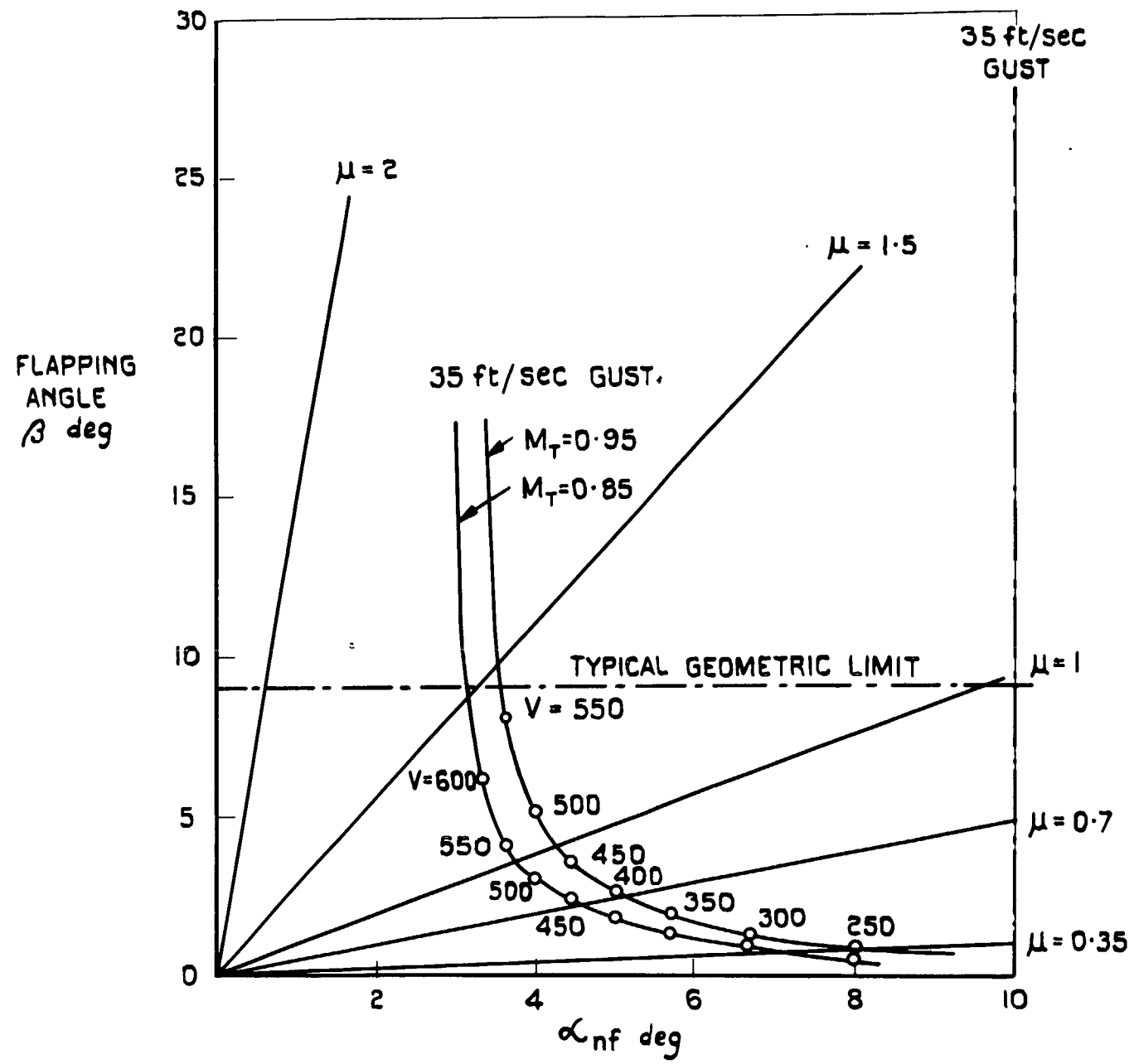

FIG. 14 EFFECT OF δ_3 HINGE ON FLAPPING RESPONSE TO CHANGE IN ANGLE OF NO-FEATHERING AXIS FREELY FLAPPING ROTOR $\delta_3 = 30°$

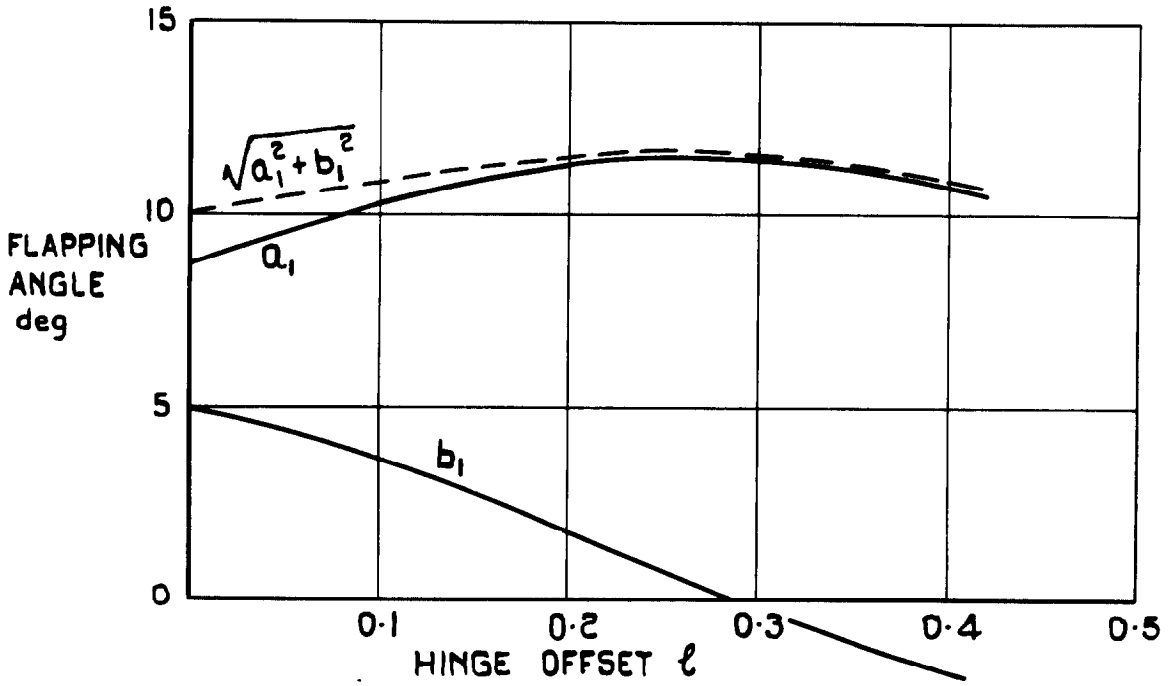

FIG. 15 FIRST HARMONICS OF BLADE FLAPPING AS A FUNCTION OF OFFSET HINGE POSITION.
($\mu = 0.4$, $\lambda = 10°$, $\theta_0 = 0$, $\gamma_0 = 6$)

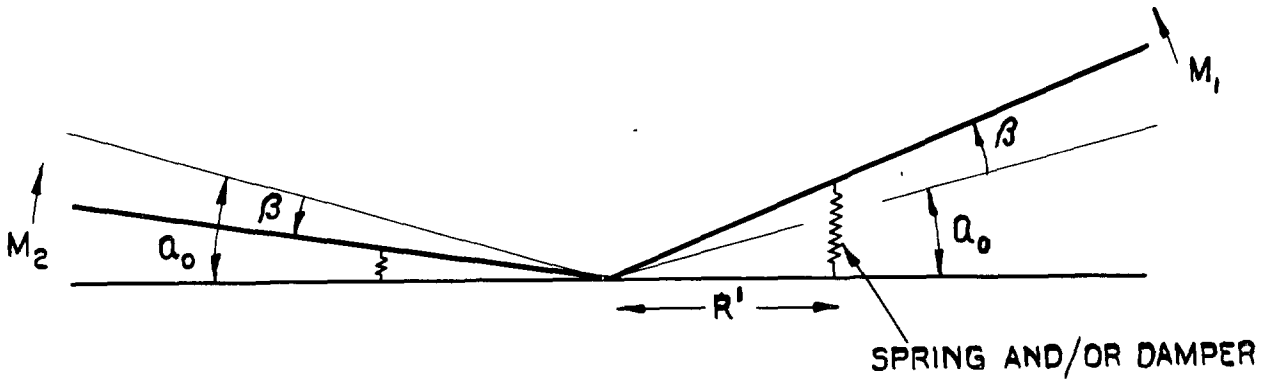

FIG. 16. ARRANGEMENT OF SPRINGS AND DAMPERS.

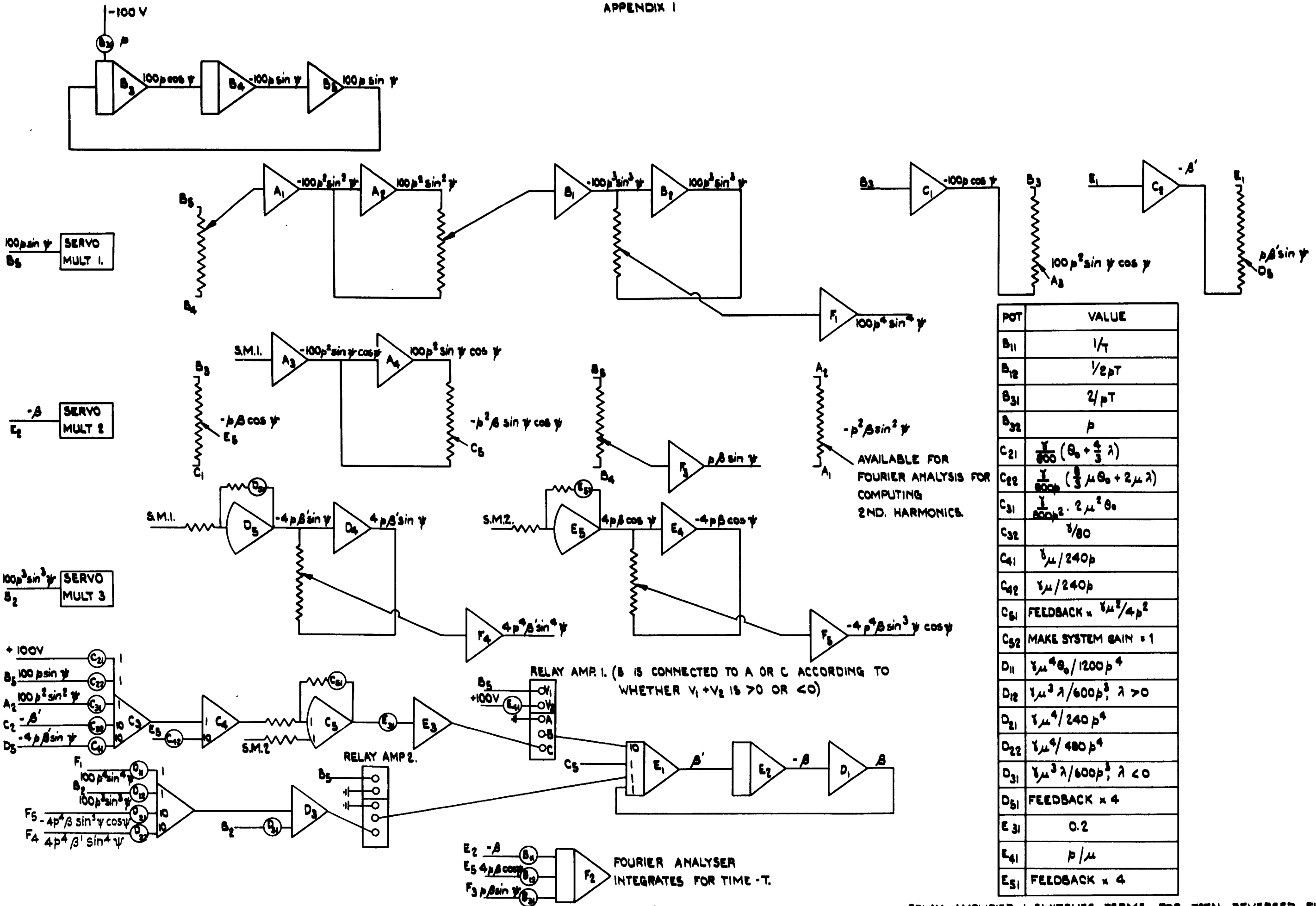

POT	VALUE
B_{11}	$1/T$
B_{12}	$1/2pT$
B_{31}	$2/pT$
B_{32}	p
C_{21}	$\frac{\gamma}{800}(\theta_0 + \frac{4}{3}\lambda)$
C_{22}	$\frac{\gamma}{800p}(\frac{8}{3}\mu\theta_0 + 2\mu\lambda)$
C_{31}	$\frac{\gamma}{800p^2}\cdot 2\mu^2\theta_0$
C_{32}	$\gamma/80$
C_{41}	$\gamma\mu/240p$
C_{42}	$\gamma\mu/240p$
C_{51}	FEEDBACK $= \gamma\mu^2/4p^2$
C_{52}	MAKE SYSTEM GAIN = 1
D_{11}	$\gamma\mu^4\theta_0/1200p^4$
D_{12}	$\gamma\mu^3\lambda/600p^3$; $\lambda > 0$
D_{21}	$\gamma\mu^4/240p^4$
D_{22}	$\gamma\mu^4/480p^4$
D_{31}	$\gamma\mu^3\lambda/600p^3$; $\lambda < 0$
D_{51}	FEEDBACK × 4
E_{31}	0.2
E_{41}	p/μ
E_{51}	FEEDBACK × 4

RELAY AMPLIFIER 1 SWITCHES TERMS FOR TOTAL REVERSED FLOW.
RELAY AMPLIFIER 2 SWITCHES TERMS FOR PARTIAL REVERSED FLOW.

ANALOGUE COMPUTER PROGRAM. FOR FREELY FLAPPING BLADE

Printed in England for Her Majesty's Stationery Office by the Royal Aircraft Establishment, Farnborough. Dd.125875. K5.

A.R.C. C.P. No.877

533.662.6 :
533.6.013.42

Wilde, E., Bramwell, A.R.S.
Summerscales, R.

THE FLAPPING BEHAVIOUR OF A HELICOPTER ROTOR AT HIGH-TIP SPEED RATIOS

April 1965

The blade flapping equation has been solved on an analogue computer taking into account the reversed flow region but neglecting stall. The fully articulated blade becomes unstable at about $\mu = 2.3$, whilst a see-saw rotor is stable up to $\mu = 5$ at least and the trends suggest that it may be stable for all values of μ. However, the response to a gust, or the equivalent change of no-feathering axis angle, is almost the same for both rotors up to about $\mu = 0.75$. For a 35 ft/sec gust at a forward speed of 200 ft/sec, and typical rotor/fuselage clearance, this represents the limiting tip-speed ratio for either rotor. The better response

A.R.C. C.P. No.877

533.662.6 :
533.6.013.42

Wilde, E., Bramwell, A.R.S.
Summerscales, R.

THE FLAPPING BEHAVIOUR OF A HELICOPTER ROTOR AT HIGH-TIP SPEED RATIOS

April 1965

The blade flapping equation has been solved on an analogue computer taking into account the reversed flow region but neglecting stall. The fully articulated blade becomes unstable at about $\mu = 2.3$, whilst a see-saw rotor is stable up to $\mu = 5$ at least and the trends suggest that it may be stable for all values of μ. However, the response to a gust, or the equivalent change of no-feathering axis angle, is almost the same for both rotors up to about $\mu = 0.75$. For a 35 ft/sec gust at a forward speed of 200 ft/sec, and typical rotor/fuselage clearance, this represents the limiting tip-speed ratio for either rotor. The better response

A.R.C. C.P. No.877

533.662.6 :
533.6.013.42

Wilde, E., Bramwell, A.R.S.
Summerscales, R.

THE FLAPPING BEHAVIOUR OF A HELICOPTER ROTOR AT HIGH-TIP SPEED RATIOS

April 1965

The blade flapping equation has been solved on an analogue computer taking into account the reversed flow region but neglecting stall. The fully articulated blade becomes unstable at about $\mu = 2.3$, whilst a see-saw rotor is stable up to $\mu = 5$ at least and the trends suggest that it may be stable for all values of μ. However, the response to a gust, or the equivalent change of no-feathering axis angle, is almost the same for both rotors up to about $\mu = 0.75$. For a 35 ft/sec gust at a forward speed of 200 ft/sec, and typical rotor/fuselage clearance, this represents the limiting tip-speed ratio for either rotor. The better response

of the see-saw rotor, however, makes it possible to increase the limiting tip-speed ratio by some form of flapping restraint. This has been investigated by considering the effects of springs and dampers, and offset and δ_3-hinges.

of the see-saw rotor, however, makes it possible to increase the limiting tip-speed ratio by some form of flapping restraint. This has been investigated by considering the effects of springs and dampers, and offset and δ_3-hinges.

of the see-saw rotor, however, makes it possible to increase the limiting tip-speed ratio by some form of flapping restraint. This has been investigated by considering the effects of springs and dampers, and offset and δ_3-hinges.

Published by
HER MAJESTY'S STATIONERY OFFICE
To be purchased from
49 High Holborn, London W.C.1
423 Oxford Street, London W.1
13A Castle Street, Edinburgh 2
109 St. Mary Street, Cardiff
Brazennose Street, Manchester 2
50 Fairfax Street, Bristol 1
35 Smallbrook, Ringway, Birmingham 5
80 Chichester Street, Belfast 1
or through any bookseller

C.P. No. 877

S.O. CODE No. 23-9016-77